trends

Applications of circular dichroism in protein and peptide analysis

Norma J. Greenfield
UMDNJ-Robert Wood Johnson Medical School, 675 Hoes Lane, Piscataway, NJ 08854-5635, USA

This review discusses several useful applications of circular dichroism as a tool for analyzing properties of proteins. The following topics are discussed: (1) protein–ligand interactions; (2) thermodynamics of protein folding; (3) conformational transitions and protein aggregation; (4) folding intermediates; (5) kinetics of protein folding. Specific examples are given to illustrate each application. ©1999 Elsevier Science B.V. All rights reserved.

Keywords: Circular dichroism; Protein-folding; Protein–ligand binding; Thermodynamics

1. Introduction

Circular dichroism (CD) is a valuable spectroscopic technique for studying protein structure in solution because many common conformational motifs, including α-helixes, β-pleated sheets, poly-L-proline II-like helices and turns, have characteristic far UV (178–250 nm) CD spectra. For example, α-helices display large CD bands with negative ellipticity at 222 and 208 nm, and positive ellipticity at 193 nm, β-sheets exhibit a broad negative band near 218 nm and a large positive band near 195 nm, while disordered extended chains have a weak broad positive CD band near 217 nm and a large negative band near 200 nm. The spectrum of a protein is basically the sum of the spectra of its conformational elements, and thus CD can be used to estimate secondary structure. In addition, the chromophores of the aromatic amino acid proteins are often in very dissymmetric environments resulting in distinctive CD spectra in the near UV (250–300 nm), which can serve as useful probes of protein tertiary structure. Recently several articles [1–3] have compared and evaluated most of the currently available computer methods for analyzing CD spectra to obtain the secondary structure of proteins, and thus this topic will not be discussed here.

Circular dichroism, however, has many more facets than simply being a tool to estimate protein structure. For example, it is an excellent technique for determining the thermodynamics and kinetics of protein folding and denaturation and is unsurpassed for following the effects of mutations on protein folding and stability. In addition, it can be an excellent tool for following protein–ligand interactions. As sophisticated mathematical programs for fitting nonlinear equations and deconvoluting sets of curves using personal computers have become increasingly available, the analysis of thermodynamic and kinetic experiments, which can be performed by following changes in CD spectra, have become much simpler, increasing the usefulness of the technique.

It would be impossible to do a complete review of all of the recent applications involving CD spectroscopy. For example, in the last 10 years there have been more than 1500 papers published in the *Journal of Biological Chemistry* alone, where CD was used to study various aspects of protein and nucleic acid chemistry. This review will therefore focus on several specific applications that illustrate of the general usefulness of CD as an analytical tool. The following topics will be discussed: (1) protein–ligand interactions; (2) thermodynamics of protein folding; (3) conformational transitions and protein aggregation phenomena; (4) folding intermediates; and (5) kinetics of protein folding. Specific examples will be used to illustrate each application.

2. Protein–ligand interactions

Circular dichroism can be used to follow protein–ligand interactions and protein denaturation because CD is a quantitative technique. Like other optical measurements, CD measurements obey Beer's law:

0165-9936/99/$ – see front matter
PII: S0165-9936(98)00112-5

the CD spectrum of each component in a solution is directly proportional to its concentration, and the total spectrum represents the sum of all the contributing spectra. Thus, the change in the CD spectrum of a protein upon addition of a ligand, denaturant or heat is directly proportional to the amount of protein changed by the perturbation.

Circular dichroism has been used to study protein–ligand interactions since the instrumentation first became available in the late 1960s [4]. Circular dichroism can be used to follow the binding of ligands to proteins, peptides and nucleic acids provided one of two criteria is fulfilled. Either the binding of ligand must bind in an dissymmetric fashion that induces *extrinsic* optical activity in the chromophores of the bound ligand, or the binding must result in a conformational change in the macromolecule that results in a change in its *intrinsic* CD spectrum. Before efficient algorithms for solving nonlinear equations became widely available, it was usually necessary to linearize the binding equations to obtain binding constants from CD data (reviewed in [5]). Today it is usual to fit the nonlinear binding equations directly using commercial programs such as SigmaPlot®, Origin®, GraphPad® and PsiPlot®, among others, which use fitting techniques such as the Levenberg–Marquardt algorithm [6] to estimate the constants which best fit the data.

2.1. Extrinsic effects

When highly chromatic ligands bind to proteins they may generate large CD bands, called Cotton effects, in the region of their absorbance spectrum if they bind in a dissymmetric fashion. The change in ellipticity as a function of substrate concentration can be used to estimate the binding constants. For example, assume a ligand with concentration $[L_i]$ binds to a protein with a concentration $[P_o]$, with n equivalent binding sites where $[LP_i]$ is the concentration of protein–ligand complex formed. The equilibrium constant, K, obeys the following equation:

$$K = ([LP_i])/([L_i]-n[LP_i])([P_o]-[LP_i]) \quad (1)$$

The change in ellipticity, θ_i, due to complex formation is directly proportional to $[LP_i]$. When all of the protein has bound ligand, $\theta_i = \theta_{max}$

$$[LP_i] = ([P_o])(\theta_i/\theta_{max}) \quad (2)$$

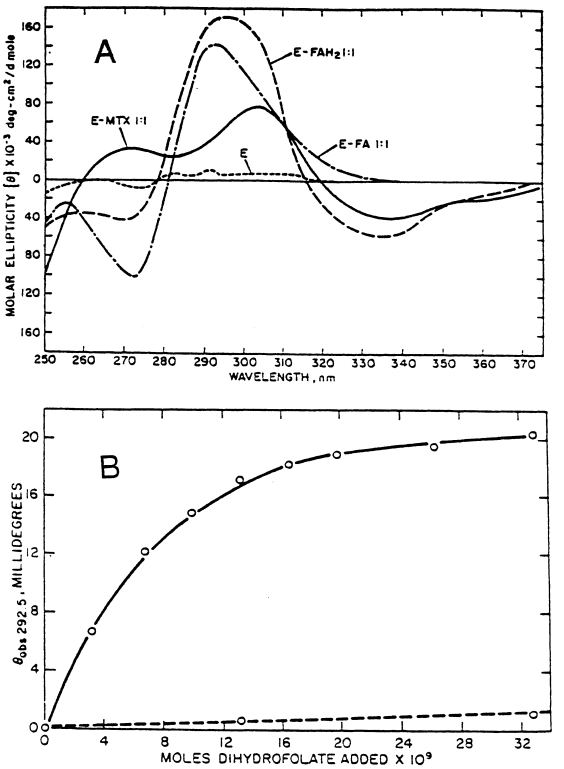

Fig. 1. (A) The molar circular dichroism of dihydrofolate reductase and 1:1 complexes with dihydrofolate (dashed line), folate (dot-dashed line) and methotrexate (solid line). (B) The increase in ellipticity at 292.5 nm as a function of dihyrofolate concentration: (solid line) enzyme plus dihydrofolate, (dashed line) dihydrofolate alone. Reprinted with permission from [7]; © (1972) American Chemical Society.

$$\theta_i = \theta_{max}\{(1 + K[P_o]/n + K[P_o])/2K[P_o] - \{((1 + K[L_i]/n + K[P_o])/2K[P_o])^2 - ([L_i]/n[P_o])\}^{1/2}\} \quad (3)$$

By fitting Eq. 3 to the raw data, the binding constant of the ligand for the protein and the number of binding sites can be estimated. To illustrate, when folates and nucleotides bind to dihydrofolate reductase large CD bands are induced [7]. Fig. 1A shows the extrinsic Cotton effects induced in the near UV when dihydrofolate, folate and methotrexate bind to dihydrofolate reductase from *Escherichia coli*, and Fig. 1B shows the change in ellipticity as a function of added dihy-

drofolate. The data were used to determine a binding constant of 1.1 μ*M*.

As well as being used to study the interactions of substrates and inhibitors with enzymes, extrinsic Cotton effects have been used to study protein–ligand interactions in diverse systems. For example, they have been used to study the binding of cofactors to proteins including the binding of nucleotides to lactic dehydrogenase [8], ATP to GroEL [9], pyridoxal phosphate to tryptophan synthase [10] and the binding of retinol to interphotoreceptor retinol binding protein [11]. In addition extrinsic CD bands have been employed to study the interactions of drugs with bovine serum albumin (e.g. [12]) and the interactions of DNA binding proteins with DNA (e.g. [13]).

2.2. Intrinsic effects

The binding of ligands to proteins often results in conformational transitions. The resultant change in the *intrinsic* ellipticity of the backbone amides caused by the conformational change can also be used to obtain the ligand binding constants. For example, divalent cations are effectors in a many biological systems that often induce large conformational changes in target proteins. For example, Ca^{2+} ion binding to the muscle regulatory protein, troponin C, induces an increase in ellipticity due to a stabilization of α-helical regions of the protein. Johnson and Potter [14] showed that CD could distinguish two classes of Ca^{2+} binding sites in troponin C, with high and low affinity. Calcium binding to the low affinity site regulates muscle contraction. Fig. 2 illustrates how the change in ellipticity of troponin C (TnC) as a function of free calcium concentration can be used to obtain the calcium binding constants for the high and low affinity sites, k_{a1} and k_{a2} [15]. Data obtained with skeletal muscle TnC, TnC expressed in *E. coli*, and a mutant TnC lacking a helical segment at the N-terminus (the N-helix) are illustrated. Chelators that bind Ca^{2+} were used as buffering agents so that the free Ca^{2+} concentration was fixed at the desired concentrations. The changes in ellipticity at 222 nm as a function of free Ca^{2+} concentration were normalized to a scale of 0 (no Ca^{2+}) to 1 (saturating Ca^{2+}) and fit to the sum of two Hill equations:

$$\theta_i = (a_1 k_{a1}^{H_1}[C_i]^{H_1})/(1 + k_{a1}^{H_1}[C_i]^{H_1}) + (a_2 k_{a2}^{H_2}[C_i]^{H_2})/(1 + k_{a2}^{H_2}[C_i]^{H_2}) \quad (4)$$

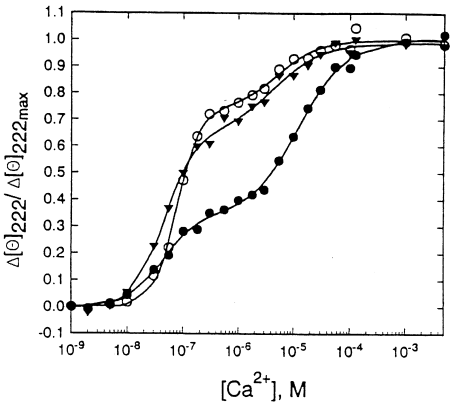

Fig. 2. The increase in ellipticity of troponin C (TnC) at 222 nn, due to increased α-helical content, as a function of free Ca^{2+} concentration. ▲, muscle TnC; ○, wild type TnC expressed in *E. coli*; ●, recombinant TnC missing the first 14 N-terminal residues. Ellipticities at 222 nm are normalized to a scale of 0 (no Ca^{2+}) to 1 (saturating Ca^{2+}). The points are the raw data, and the lines are the data fitted by the sum of two Hill equations. Reprinted with permission from [15]; © (1994) The American Society for Biochemistry and Molecular Biology, Inc.

where θ_i is the change in ellipticity at 222 nm observed when calcium binds to TnC, H_1 and H_2 are the Hill constants and a_1 and a_2 are the molar absorptivities for the spectral change caused by calcium binding to the high and low affinity sites, respectively, and $[C_i]$ is the free calcium concentration. Initial estimate of a_1, a_2, H_1, H_2, k_{a1} and k_{a2} were made and the equations were fit using the Levenberg–Marquardt algorithm [6] implemented in the commercial program SigmaPlot. The deletion of the N-helix caused a threefold decrease in the binding of calcium to the regulatory site of TnC [15].

There are many other classes of protein–ligand interactions that result in conformational changes. For example, DNA binding to DNA transcription factors results in an increase in helical content of the transcription factor. These factors often contain α-helical coiled-coils or helix-loop-helix motifs, which serve as dimerization domains, and a relatively unstructured basic region which binds to DNA. Upon binding to the DNA the basic region assumes a helical conformation. Fig. 3 illustrates the increase in ellipticity when two muscle helix-loop-helix regulatory factors, E47 and MyoD bind to an oligonucleotide containing the creatine enhancer site [16].

Another interesting class of protein–ligand interactions, resulting in conformational changes, is the bind-

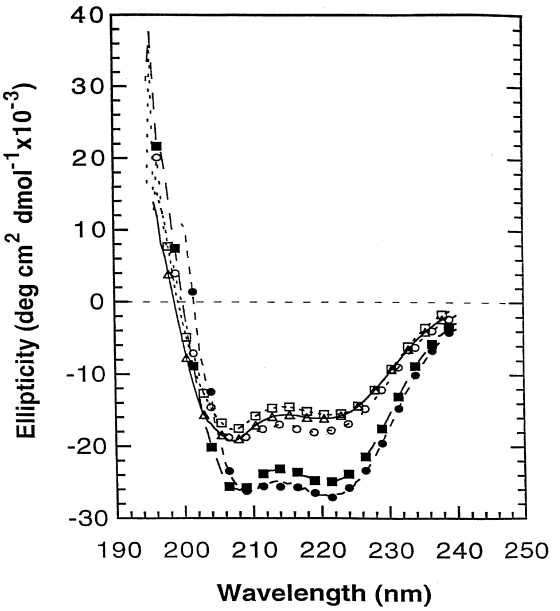

Fig. 3. The backbone ellipticity of two muscle DNA transcription factors: ○, E47 and □, MyoD, and △, a chimera, MyoEL, in which the loop region of MyoD has been replaced by that of E47. The CD spectra of all three proteins are similar and are characteristic of a partially helical structure. Addition of an oligonucleotide containing the creatine kinase enhancer site to ●, E47 or ■, MyoD increases negative ellipticity at 222 and 208 nm characteristic of α-helices, because the basic region folds upon binding to DNA. Reprinted with permission from [16]; © (1998) The American Society for Biochemistry and Molecular Biology, Inc.

ing of heparin to diverse proteins including the amino-terminal domain of fibronectin [17], hepatocyte growth factor [18], the amyloid precursor protein of Alzheimer's disease [19] and annexin [20] among others. The binding of heparin has very different effects, depending on its target. CD studies show that a peptide derived from the amyloid precursor protein, APP416–447 shifts towards an α-helical conformation in the presence of heparin. In contrast, the Ca^{2+}-dependent binding of heparin to annexin caused a large decrease in its α-helical content from approximately 44 to 31%, a small decrease in the β-sheet content from approximately 27 to 24%, and an increase in the unordered structure from 20 to 29%. A peptide fragment corresponding to the heparin binding site of hepatocyte growth factor changes from a random structure to a β-sheet-like structure upon heparin binding, which results in the oligomerization of the growth factor.

3. Thermodynamics of protein folding

Following changes in the optical activity of a protein or polypeptide as a function of temperature or denaturant is a very convenient method of obtaining the thermodynamics of folding. Indeed, the major application of CD today is the determination of the thermodynamics of protein folding and the effects of mutations on protein stability. The equations describing the thermodynamics of structural stability and cooperative folding behavior in proteins have been reviewed by Freire [21]. The applications of CD to studies of protein folding have been recently reviewed by Kelly and Price [22].

3.1. Thermodynamic parameters of folding from thermal denaturation and renaturation studies

Essentially the use of CD to follow protein denaturation depends on the fact that the change in ellipticity is directly proportional to the change in concentration of native and denatured forms. The observed ellipticity of a protein, θ_{obs}, changes when it unfolds. When the protein is fully folded $\theta_{obs} = a_1$ and when it is fully unfolded $\theta_{obs} = a_2$. In the case of a monomeric protein, the equilibrium constant of folding, K = folded/unfolded. If we define α as the fraction folded at a given temperature then

$$K = \alpha/(1-\alpha) \tag{5}$$

$$\Delta G = nRT\ln K \tag{6}$$

where ΔG is the free energy of folding and R is the gas constant = 1.987 cal/mol.

$$\Delta G = \Delta H - T\Delta S \tag{7}$$

where ΔH is the enthalpy of folding and ΔS is the entropy of folding. T_M is the observed midpoint of the thermal transition. At the T_M, $K = 1$, therefore $\Delta G = 0$ and $\Delta S = \Delta H/T_M$. Solving these equations we obtain:

$$K = \exp\{(\Delta H/RT)((T/T_M)-1)\} \tag{8}$$

$$\alpha = K/(1+K) \tag{9}$$

$$\theta_{obs} = (a_1 - a_2)\alpha + a_2 \tag{10}$$

To calculate the values of ΔH and T_M that best describe the folding curve, initial values of ΔH, T_M,

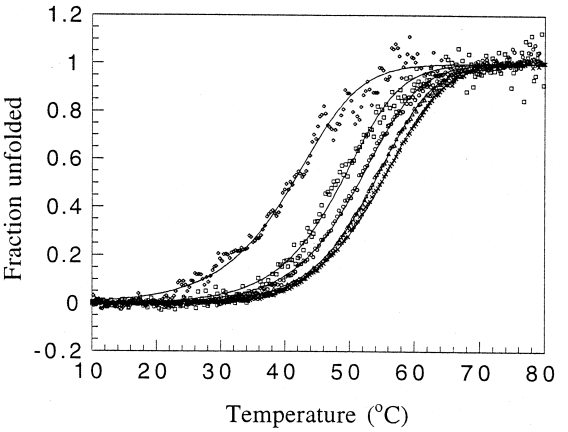

Fig. 4. The change in fraction folded of GCN4 as a function of temperature and peptide concentration. The concentrations range from 1 μ*M* with the lowest T_M to 20 μ*M* with the highest T_M. The enthalpy of unfolding was 35.0 ± 1.1 kcal/mol (monomer) which compared to that of 34.7 ± 0.3 kcal/mol measured by calorimetry. Reprinted with permission from [25]; © (1993) American Chemical Society.

a_1 and a_2 are estimated, and Eq. 10 is fitted to the experimentally observed values of the change in ellipticity as a function of temperature, by a curve fitting routine such as the Levenberg–Marquardt algorithm [6]. Since at $K = 1$, $\Delta G = 0$, the entropy of folding can therefore be calculated using Eq. 4 where $\Delta S = \Delta H / T_M$. The free energy of folding at any other temperature can then be calculated using Eq. 4. Note that this treatment ignores changes in heat capacity, ΔC_p, when a protein unfolds, but equations have been developed that include that term [23]. Similar equations can be used to estimate the thermodynamics of folding of proteins and peptides that undergo folded multimer to unfolded monomer transitions (reviewed in [24]). The free energy of folding may also be calculating from the concentration dependence of CD spectra, if changes in association state are accompanied by changes in conformation.

Fig. 4 illustrates how changes in ellipticity as a function of temperature and concentration have been used to determine the enthalpy of folding of the GCN4 transcription factor, which undergoes a two-state transition between a folded two-stranded α-helical coiled-coil and a monomeric disordered state [25]. The values for the enthalpy of the folding transition, determined from the changes in ellipticity as a function of temperature agreed with the values obtained from scanning calorimetry.

3.2. Thermodynamic parameters of protein folding using denaturants

In some cases thermal folding and unfolding studies are impractical. The protein may have a very high T_M, or may aggregate and precipitate upon heating. In these cases denaturants, such as urea or guanidine-HCl, may be added to a protein or peptide to induce unfolding. One obtains K at each concentration of denaturant by assuming that the protein is native in the absence of denaturant, and fully unfolded when there is no further change in ellipticity upon addition of higher concentrations of perturbant. In each case, K, the equilibrium constant of folding is determined from

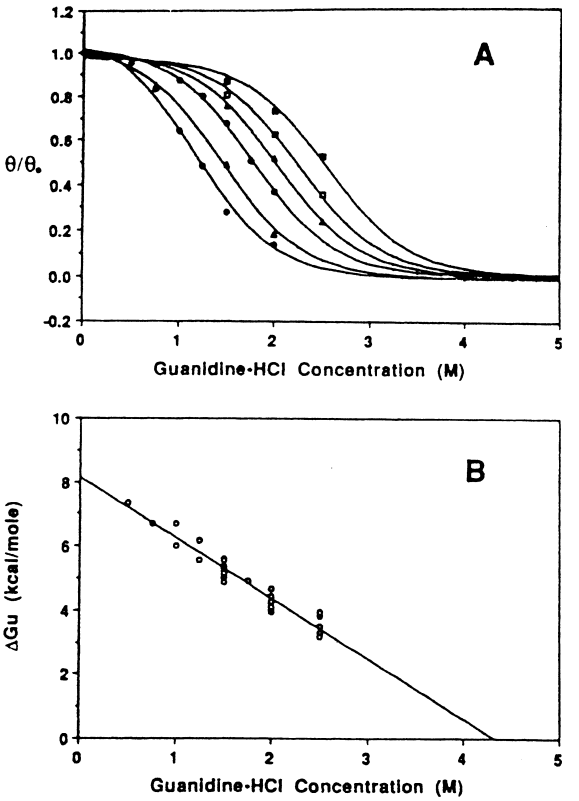

Fig. 5. (A) Concentration dependence of the guanidine hydrochloride denaturation of a coiled-coil model peptide. Concentrations of the peptide were ●, 48 μ*M*; △, 131 μ*M*; ○, 213 μ*M*; ▲, 592 μ*M*; □, 888 μ*M* and ■, 1345 μ*M*. (B) Plot of linear dependence of ΔG of unfolding on the concentration of guanidine hydrochloride at different concentrations of the peptide, extrapolated to zero to determine the free energy of unfolding in the absence of denaturant. The correlation coefficient for the regression line was 0.94. Reprinted with permission from [26]; © (1992) The American Society for Biochemistry and Molecular Biology, Inc.

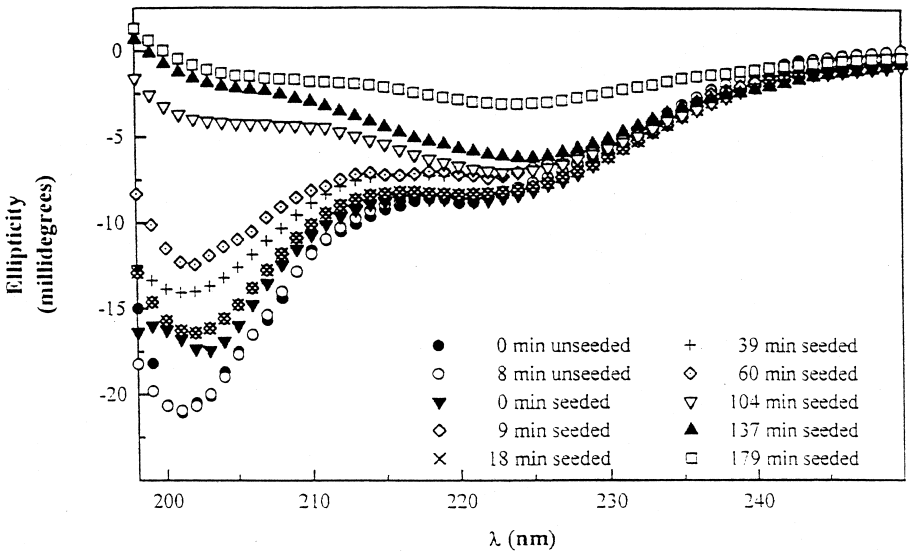

Fig. 6. Time-dependent aggregation of islet amyloid polypeptide (IAPP) seeded with IAPP which had been subjected to prolonged glycosylation to produce advanced glycosylation end products (AGE). After seeding the peptide went from a conformation which was predominantly random with a small amount of α-helix to one with a high β-content, followed by aggregation and precipitation out of solution. Reprinted with permission from [30]; © (1998) FEBS.

the ellipticity observed at each concentration of denaturant.

$$K = \alpha/(n[C]^{n-1})(1-\alpha)^n \quad (11)$$

where

$$\alpha = (\theta_{obs}-a_2)/(a_1-a_2) \quad (12)$$

α, a_1 and a_2 have the same definitions as in the case of thermal unfolding above. $[C]$ is the total concentration of protein monomers. The free energy of folding is evaluated at every concentration of denaturant using the equation $\Delta G = -nRT\ln K$. The free energies are plotted as a function of denaturant and extrapolated to zero denaturant to obtained the free energy of folding of the native material. Hodges and coworkers have used this approach to study the contributions of hydrophobic and charged residues to the stability of designed coiled-coil α-helices. Fig. 5 illustrates the determination of the free energy of folding of a coiled-coil model peptide from a guanidine denaturation study [26]. It should be noted that one may obtain different apparent ΔGs of folding when different denaturants are employed because some denaturants, such as solutions of guanidine-HCl, which have a high ionic strength, disrupt salt bridges in proteins, while others, such as urea, which is uncharged, have a lesser effect on protein charge–charge interactions.

4. Conformational transitions

While CD is most usually used to study transitions from a folded to an unfolded state, recently it has been found that certain systems undergo transitions involving changes from an α-helical to a β-pleated sheet conformation (or vice versa). Conformational transitions may be followed by oligomerization of the protein and/or aggregation and precipitation. Such conformational changes can have important clinical consequences as it is felt that such transitions may be involved in the pathology of diseases such as scrapie, 'mad cow disease' and Alzheimer's disease. CD has been used to follow conformational transitions in prions (e.g. [27]), the Alzheimer's β-amyloid peptide (e.g. [28]) and amylin, an amyloid peptide seen in the pancreatic islets in patients with diabetes (e.g. [29]). Fig. 6 illustrates conformational changes of islet amyloid polypeptide after seeding with peptide modified with advanced glycosylation end products [30]. The peptide rapidly goes from a conformation that is predominantly random, with a small amount of α-helix, to a conformation with considerable β-structure. After the structural transition, the peptide associates into fibrils and precipitates out of solution.

5. Folding intermediates

Often when proteins or peptides fold or unfold, the process is not a two-state transition between the native and totally disordered forms; there are intermediate states. These states may be transient, and may be observed during kinetic measurements of folding or unfolding, or they may be stable intermediates, seen when the peptide is subject to denaturing conditions, such as high temperatures, or exposure to urea, guanidine or detergents. These states may be partially folded, with defined tertiary structures, or may be so called molten globules. The term molten globule was first introduced by Ptitsyn and coworkers (for reviews see [31,32]) to describe a compact state with native-like secondary structure but slowly fluctuating tertiary structure.

CD can often be used to detect and quantify the intermediate states. For example, some 'molten globule' folding intermediates exhibit large CD signals in the far UV arising from secondary structural elements such as α-helices. The molten globule folding intermediates, however, display almost none of the near UV CD bands arising from tertiary structural interactions of aromatic groups, which are often seen in the spectra of native proteins. A classic example of a protein with a partially folded molten globule state is α-lactalbumin (for a review see [33]).

It is often useful to be able to quantify the contribution of multiple states to the unfolding of a protein. There are several published algorithms that allow a set of spectra which are obtained under different conditions to be deconvoluted into a smaller number of basis curves. The original curves are a linear combination of the basis curves. The amount of each basis curve contributing to each spectrum is then quantified. Two widely used algorithms for deconvoluting sets of CD spectra into basis curves are singular value decomposition (SVD) (reviewed in [34]) and the convex constraint algorithm (CCA) of Perczel et al. [35].

The CCA and SVD methods have been applied to diverse problems in protein chemistry. For example, Greenfield and Hitchcock-DeGregori [36] used CCA to quantify the contribution of a molten globule-like state to the unfolding of a designed coiled-coil peptide. At 0°C the peptide was 100% α-helical and had a pronounced positive band at 280 nm arising from its tyrosine residue. When heated from 0 to 50°C, the peptide lost all of its ellipticity in the near UV, while retaining more than 75% of its α-helical content, suggesting that it went from a native to a molten-globule state before completely dissociating to give disordered chains. Deconvolution of the CD data obtained in the far UV, as a function of temperature, showed that at least three basis spectra were needed to fit the data. Safer et al. [28] similarly used the CCA algorithm to examine the thermal stability and conformational transitions of scrapie amyloid (prion) protein, PrP27–30. CCA deconvolution of the CD spectra of the solvent-exposed and rehydrated solid state PrP27–30 identified five common spectral components. The loss of infectivity quantitatively correlated with a decreasing proportion of native, β-sheet-like secondary structure component, an increasing amount of an α-helical component, and an increasingly disordered tertiary structure. In a recent example, Konno [37] has used SVD to analyze and quantify different conformational states of acid denatured cytochrome C.

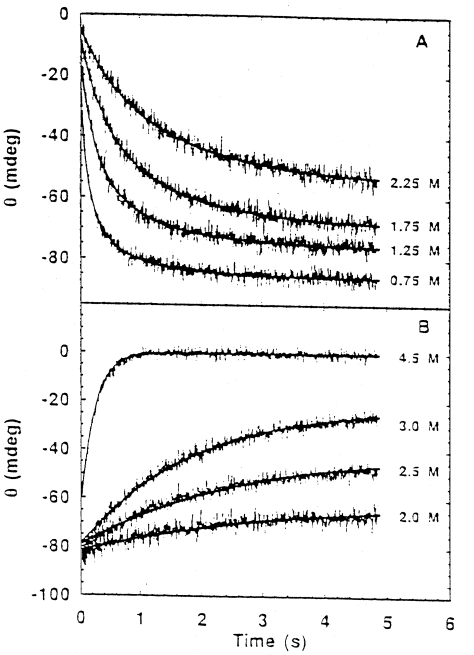

Fig. 7. Kinetics of refolding (A) and unfolding (B) traces at various final guanidine-HCl concentrations and constant peptide concentrations of the GCN4-P1 monitored by the change in ellipticity at 222 nm at pH 7.0 and 5°C. Solid lines represent global fits to the model of a native dimer dissociating to give two unfolded chains. Reprinted with permission from [39]; © (1995) American Chemical Society.

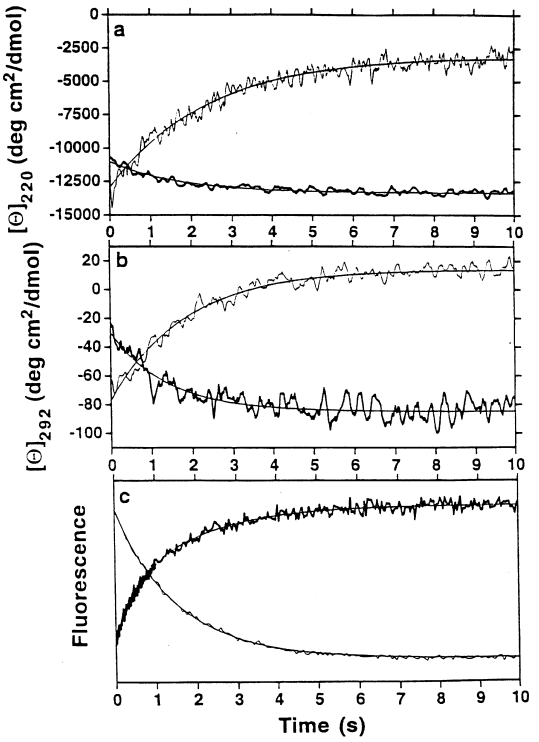

Fig. 8. Kinetic curves of the unfolding (thin line) and refolding (thick line) of RNAse HI as monitored by (A) far UV CD due to the secondary structure at 220 nm, (B) near UV at 292 nm due to tertiary interactions, and (C) fluorescence (excitation at 280 nm and emission over 300 nm). Only a single exponential process was detected for unfolding using all three probes. For refolding, the far UV CD value largely recovered within 50 ms of the stopped-flow mixing dead time (burst phase). This phase was followed by either one phase detected by both near UV and far UV CD with a rate constant of approximately 0.5–0.6 s^{-1}. Refolding detected by fluorescence detected two phases, one with a rate constant of 1.95 s^{-1} and one with a rate constant of 0.5 s^{-1} corresponding to the phase detected by near UV CD. Reprinted with permission from [40]; © (1995) American Chemical Society.

6. Kinetics of protein folding

Besides the study of protein folding under equilibrium conditions, CD can be used to measure rapid events in protein folding and unfolding by attaching a rapid mixing device to a CD spectrometer. Stopped-flow CD has recently been reviewed by Kuwajima [38]. Stopped-flow CD can be used both to obtain the kinetic constants of folding reactions and to define the conformations of folding intermediates. Data can be collected in the far and near UV.

In an elegant study of the development of secondary structure as a function of time, Zitzewitz et al. [39] have used stopped-flow CD to characterize the folding of the GCN4-P1 peptide. This peptide is an α-helical coiled-coil comprised of the leucine zipper domain of the yeast GCN4 DNA transcription factor. The CD data obtained during guanidine-HCl induced equilibrium unfolding of this peptide were consistent with a two-state model involving the transition of a native α-helical coiled-coil dimer to an unfolded monomer. The unfolding and refolding kinetics of GCN4-P1 were monitored by stopped-flow CD a function of both peptide and denaturant concentration. The unfolding kinetics displayed single-exponential behavior, consistent with a unimolecular reaction. The refolding kinetics were dependent on both peptide and guanidine concentration and were well described by a simple bimolecular association reaction (see Fig. 7). The equilibrium constants calculated from the rate constants of folding and unfolding agreed with those obtained from the equilibrium measurements, showing that all the data were consistent with a two-state folding model.

Studies of changes in the near and far UV CD of proteins, in parallel with other spectroscopic measurements, can give valuable information about the nature of protein folding intermediates. In a recent example illustrated in Fig. 8, Yamasaki et al. [40] used stopped-flow CD and fluorescence to study the refolding of ribonuclease HI from *E. coli*. Both the unfolding and refolding processes, induced by concentration jumps of either guanidine hydrochloride (GuHCl) or urea, were studied. The peptide unfolds in a concerted two-state transition. The difference in the amplitudes of the burst phases for refolding, however, monitored by fluorescence and far and near UV CD spectra, suggest that an intermediate state exists with characteristics of a molten globule. Hydrogen exchange refolding competition combined with two-dimensional NMR revealed that the amide protons of α-helix I are the most highly protected, suggesting that α-helix I is the initial site of protein folding. The CD and NMR data showed that the intermediate state has a structure similar to that of the acid-denatured molten globule.

7. Conclusion

Circular dichroism has many interesting and exciting uses for the study of protein and polypeptide structure, folding and interactions. The power of CD as an

analytical tool is increased greatly when used in conjunction with other spectroscopic methods such as fluorescence and NMR. CD is an invaluable tool for protein and peptide scientists, interested in understanding both the fundamental basis of macromolecular interactions and the nature of diseased states caused by mutated or misfolded proteins.

Acknowledgements

I am grateful to Dr. Ernesto Freire for supplying an original copy of the graph reproduced in Figure 4 and I am indebted to Dr. Sarah E. Hitchcock-DeGregori and Dr. Barbara Brodsky for critically reading the manuscript. This work was supported by NIH Grants GM36326 to S.E.H.D. and N.J.G. and HL35726 to S.E.H.D. and by the CD facility at UMDNJ-Robert Wood Johnson Medical School.

References

[1] R.W. Woody, Methods Enzymol. 246 (1995) 34.
[2] S.Y. Venyaminov and J.T. Yang, in G.D. Fasman (Editor), Circular Dichroism and the Conformation Analysis of Biomolecules, Plenum Press, New York, 1996, p. 69.
[3] N.J. Greenfield, Anal. Biochem. 235 (1996) 1.
[4] J.H. Perrin, P.A. Hart, J. Pharm. Sci. 59 (1970) 431.
[5] N.J. Greenfield, CRC Crit. Rev. Biochem. 3 (1975) 71.
[6] D.W. Marquardt, J. Soc. Ind. Appl. Math. 11 (1963) 431.
[7] N.J. Greenfield, M.N. Williams, M. Poe, K. Hoogsteen, Biochemistry 11 (1972) 4706.
[8] R. Jaenicke, E. Gregori, M. Laepple, Biophys. Struct. Mech. 6 (1979) 57.
[9] Z.W. White, K.E. Fisher, E. Eisenstein, J. Biol. Chem. 270 (1995) 20404.
[10] H. Balk, I. Merkl, P. Bartholmes, Biochemistry 20 (1981) 6391.
[11] A.J. Adler, C.D. Evans, W.F. Stafford 3d, J. Biol. Chem. 260 (1985) 4850.
[12] V.K. Cheruvallath, C.M. Riley, S.R. Narayanan, S. Lindenbaum, J.H. Perrin, J. Pharm. Biomed. Anal. 15 (1997) 1719.
[13] M.S. Soengas, C.R. Mateo, G. Rivas, M. Salas, A.U. Acuna, C. Gutierrez, J. Biol. Chem. 272 (1997) 303.
[14] J.D. Johnson, J.D. Potter, J. Biol. Chem. 253 (1978) 3775.
[15] L. Smith, N.J. Greenfield, S.E. Hitchcock-DeGregori, J. Biol. Chem. 269 (1994) 9857.
[16] H. Wendt, R.M. Thomas, T. Ellenberger, J. Biol. Chem. 273 (1998) 5735.
[17] R. Kishore, M. Samuel, Y. Khan, J. Hand, D.A. Frenz, S.A. Newman, J. Biol. Chem. 272 (1997) 17078.
[18] H. Aoyama, D. Naka, Y. Yoshiyama, T. Ishii, J. Kondo, M. Mitsuka, T. Hayase, Biochemistry 36 (1997) 10286.
[19] S.S. Mok, G. Sberna, D. Heffernan, R. Cappai, D. Galatis, H.J. Clarris, W.H. Sawyer, K. Beyreuther, C.L. Masters, D.H. Small, FEBS Lett. 415 (1997) 303.
[20] G. Kassam, A. Manro, C.E. Braat, P. Louie, S.L. Fitzpatrick, D.M. Waisman, J. Biol. Chem. 272 (1997) 15093.
[21] E. Freire, Methods Enzymol. 259 (1995) 144.
[22] S.M. Kelly, N.C. Price, Biochim. Biophys. Acta 1338 (1997) 161.
[23] M.R. Eftink, Methods Enzymol. 259 (1995) 487.
[24] K.J. Breslauer, Methods Enzymol. 259 (1987) 221.
[25] K.S. Thompson, C.R. Vinson, E. Freire, Biochemistry 32 (1993) 5491.
[26] N.E. Zhou, C.M. Kay, R.S. Hodges, J. Biol. Chem. 267 (1992) 2664.
[27] J. Safar, P.P. Roller, D.C. Gajdusek, C.J. Gibbs Jr., Protein Sci. 2 (1993) 2206.
[28] M. Hollosi, L. Otvos Jr., J. Kajtar, A. Percel, V.M. Lee, Peptide Res. 2 (1989) 109.
[29] L.R. McLean, A. Balasubramaniam, Biochim. Biophys. Acta 1122 (1992) 317.
[30] A. Kapurniotu, J. Bernhagen, N. Greenfield, Y. Al-Abed, S. Teichberg, R.W. Frank, W. Voelter, R. Bucala, Eur. J. Biochem. 251 (1998) 208.
[31] D.T. Haynie, E. Freire, Proteins Struct. Funct. Genet. 16 (1993) 115.
[32] O.B. Ptitsyn, Trends Biochem. Sci. 20 (1995) 376.
[33] K. Kuwajima, FASEB J. 10 (1996) 102.
[34] E.R. Henry, J. Hofrichter, Methods Enzymol. 222 (1992) 679.
[35] A. Perczel, M. Hollosi, G. Tusnady, G.D. Fasman, Protein Eng. 4 (1991) 669.
[36] N.J. Greenfield, S.E. Hitchcock-DeGregori, Protein Sci. 2 (1993) 1263.
[37] T. Konno, Protein Sci. 7 (1998) 975.
[38] K. Kuwajima, in G.D. Fasman (Editor), Circular Dichroism and the Conformational Analysis of Biomolecules, Plenum Press, New York, 1969, p. 159.
[39] J.A. Zitzewitz, O. Bilsel, J. Luo, B.E. Jones, C.R. Matthews, Biochemistry 34 (1995) 12812.
[40] K. Yamasaki, K. Ogasahara, K. Yutani, M. Oobatake, S. Kanaya, Biochemistry 34 (1995) 16552.